A LETTERS JOURNAL EXPLORING
THE FRONTIERS OF PHYSICS

OFFPRINT

Periodic compression of an adiabatic gas: Intermittency-enhanced Fermi acceleration

CARL P. DETTMANN and EDSON D. LEONEL

EPL, **103** (2013) 40003

A Letters Journal Exploring the Frontiers of Physics

August 2013

EPL, **103** (2013) 40003
doi: 10.1209/0295-5075/103/40003

www.epljournal.org

Periodic compression of an adiabatic gas: Intermittency-enhanced Fermi acceleration

Carl P. Dettmann[1] and Edson D. Leonel[2]

[1] *School of Mathematics, University of Bristol - Bristol BS8 1TW, UK, EU*
[2] *Departamento de Física, UNESP - Universidade Estadual Paulista - Av. 24A, 1515, Bela Vista, CEP: 13506-900, Rio Claro, SP, Brazil*

received 3 May 2013; accepted in final form 23 August 2013
published online 11 September 2013

PACS 05.20.Dd – Kinetic theory
PACS 05.45.Ac – Low-dimensional chaos

Abstract – A gas of non-interacting particles diffuses in a lattice of pulsating scatterers. In the finite-horizon case with bounded distance between collisions and strongly chaotic dynamics, the velocity growth (Fermi acceleration) is well described by a master equation, leading to an asymptotic universal non-Maxwellian velocity distribution scaling as $v \sim t$. The infinite-horizon case has intermittent dynamics which enhances the acceleration, leading to $v \sim t \ln t$ and a non-universal distribution.

Periodically forced thermally isolated systems exhibit many interesting phenomena from stabilization [1] to exponential acceleration [2]. They are of great interest for trapped atom [3] and ion [4] experiments, as well as astrophysical problems such as transport of comets [5]. Using a spatial coordinate as the independent variable, they also describe transport in periodic structures [6]. Typically there is an unbounded growth of the energy, the phenomenon of Fermi acceleration [7] (FA). Very recently, many researchers have sought analytical descriptions of energy distributions in such systems [8–11]. In rather general circumstances, a Fokker-Planck (FP) equation can be derived, incorporating the average and variance of the work per period [8]. The first example in [8], extensively investigated elsewhere [9–15], consists of a particle, or equivalently gas of non-interacting particles, moving freely in a container ("finite billiard") or amongst obstacles ("Lorentz gas") with oscillating boundary but fixed volume. Our main aim is to investigate forced systems with oscillating volume, developing methods (applicable to general classes of FA systems) to characterise and tame the resulting wild oscillations in the energy distribution. We exhibit contrasting features of chaotic and intermittent regimes, including the paradoxical effect that, in the intermittent case, fewer collisions lead to greater acceleration.

Periodically oscillating billiard(-like) models exhibiting FA include the 1D bouncer [16] and stochastic simplified Fermi-Ulam [10] models. In the latter (and often elsewhere), the simplifying assumption of the static-wall approximation (SWA) was used, where the boundaries are fixed (hence trivially having fixed volume) but the particle changes its velocity as if they were moving. Many oscillating two-dimensional billiards have also been considered and lead to FA. It is conjectured that this includes all chaotic geometries [14,15], as well as the ellipse [17]. The breathing case (fixed shape) has been studied in detail [18], leading to a slower growth of velocity than that of other typical models. FA is normally prevented by dissipation in the dynamics, although there are scaling laws relating the final energy to the strength of the dissipation [19].

Jarzyński and Świątecki [12], showed, using moments, that for fixed-volume time-dependent billiards, the eventual distribution of velocities is exponential, in contrast to the Gaussian distribution of an equilibrium gas; this was confirmed numerically in ref. [20]. Jarzyński [21] then described an FP equation approach for a slowly varying billiard (or fast particle) giving an explicit calculation of the rates of increase of the energy and its variance; this was later applied, with some further approximation and difficulties due to dynamical correlations, to a system with oscillating volume [22]. Bouchet, Cecconi and Vulpiani [23] applied a linear Boltzmann equation in an astrophysical context to obtain an exponential velocity distribution. More recent innovations have included a hopping-wall approximation replacing the SWA [13], and a Chapman-Kolmogorov equation replacing an FP equation [10]. Here

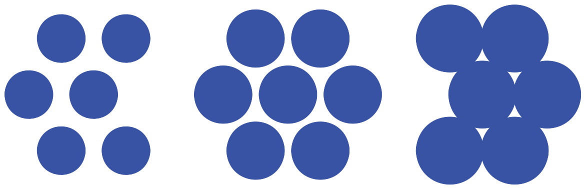

Fig. 1: (Colour on-line) The triangular Lorentz gas consists of a particle moving freely except for reflections with a periodic array of obstacles. Transport consists of three regimes: infinite horizon (left) with unbounded free path length, finite horizon (center) with bounded free paths but overall diffusion, and confined (right).

we retain the simpler FP approach, but treat the wall collisions exactly. Many of these techniques are also relevant to stochastically moving boundaries [11,24].

Our model is a two-dimensional Lorentz gas, a collection of circular scatterers in an extended domain. Fixed random [25] and periodic [26] scatterer arrangements have been widely studied for the last century. In the periodic case, the transport regimes are infinite horizon (IH), finite horizon (FH) and confined (C) as illustrated in fig. 1. In the IH and FH cases a particle can diffuse to arbitrarily great distances; Green-Kubo formulae [27] express the diffusion coefficient as the infinite time integral of the velocity autocorrelation function $\langle v(t)v(0)\rangle$. In the FH case this is believed to decay as $\exp(-Ct)$, while in the IH case as C/t. Thus, for IH the integral diverges, leading to logarithmic superdiffusion [26]. In both cases the collision dynamics is strongly chaotic, and the anomalous IH diffusion is due to long flights.

We place the scatterers on a triangular lattice, with each unit cell having unit area, so the distance between the centres of neighbouring scatterers is $(4/3)^{1/4}$. The triangular Lorentz gas is IH for $r < r_H = (3/64)^{1/4} \approx 0.465$, FH for $r_H < r < r_I = (1/12)^{1/4} \approx 0.537$, at which the scatterers start to intersect, and confined (C) for $r_I < r < r_B = (4/27)^{1/4} \approx 0.620$ at which point the dynamics is blocked as there is no space outside the scatterers. The area available to a billiard particle $\mathcal{A}(r)$ is

$$\begin{cases} 1-\pi r^2, & r \le r_I, \\ 1-r^2\left(\pi - 6\arccos\dfrac{r_I}{r} + 6\sqrt{\dfrac{r_I^2}{r^2}-\dfrac{r_I^4}{r^4}}\right), & r \ge r_I. \end{cases} \tag{1}$$

Here we consider time-dependent scatterers, with radius $r(t) = R + A\sin t$ and boundary velocity $u(t) = r'(t) = A\cos t$. There are several scenarios depending on $R_\pm = R \pm A$. Our {I, F, C} notation indicates what regimes exist as time passes, so IFC indicates that between infinite and confined times there is a finite horizon:

- I infinite (horizon) $R_+ < r_H$;
- IF infinite, finite $R_- < r_H < R_+ < r_I$;
- IFC infinite, finite, confined $R_- < r_H < r_I < R_+$;
- F finite $r_H < R_- < R_+ < r_I$;
- FC finite, confined $r_H < R_- < r_I < R_+$;
- C confined $r_I < R_-$.

Reference [9] presents some discussion of a IF model (with fixed volume), denoting it as "dynamically infinite horizon". For the numerical simulations we choose $A = 0.03$, which allows all the above cases except IFC. A Lorentz gas on a square lattice has no finite horizon, and so exhibits regimes I, IC and C.

We first discuss FA for the finite or confined geometries. The billiard particles move freely, colliding with the scatterers according to [18]

$$\mathbf{v}_+ = \mathbf{v}_- + 2\mathbf{n}(u - \mathbf{n}\cdot\mathbf{v}_-), \tag{2}$$

where $\mathbf{v}_+$ ($\mathbf{v}_-$) is the velocity immediately after (before) the collision, $\mathbf{n}$ is an outward unit normal at the point of collision, and we use $v_\pm = |\mathbf{v}_\pm|$. The incoming angle θ with respect to the normal satisfies $-\mathbf{n}\cdot\mathbf{v}_- = v_-\cos\theta$. If a particle with $v_- < u$ is overtaken by the scatterer then $\theta > \pi/2$. We define $\theta \ge 0$ so there is a $1:1$ relation between θ and the outgoing speed v_+, thus each $\theta > 0$ corresponds to two incoming directions. Equation (2) gives

$$v_+^2 = \mathbf{v}_+\cdot\mathbf{v}_+ = v_-^2 + 4uv_-\cos\theta + 4u^2. \tag{3}$$

Thus, the change in speed has the same sign as u and is of magnitude up to $2|u|$.

This system exhibits FA, and almost all initial conditions to lead to unbounded speed; after sufficient time, v exceeds all velocity scales set by the problem, including $|u|$ and the lattice spacing times the oscillation frequency. Thus, the particles are effectively in a Lorentz gas with slowly varying radius, and as in the static case, having exponential decay of time correlation functions. The only quantity not randomised by the dynamics at short times is v, a constant of motion for the static case.

Thus, we may describe the system by a spatially homogeneous distribution function $f(v,t)\delta v$ giving the probability of observing a particle with speed in the interval $[v, v+\delta v]$ at time t, hence normalised so

$$\int_0^\infty f(v,t)\mathrm{d}v = 1 \tag{4}$$

for all t. The probability of finding the particle in a region of the full phase space is, under this assumption, $f(v,t)\delta v\frac{\delta\psi}{2\pi}\frac{\delta x\delta y}{\mathcal{A}}$, where ψ denotes the direction of the velocity, including the relevant normalisation factors. Here, and often later, the time dependence of r (and hence $\mathcal{A}$) has been suppressed for simplicity.

The distribution $f(v,t)$ evolves due to collisions with the scatterers, which make small changes of order u to the speed. The collisions depend on one distribution function and the known position and velocity of the scatterers, so the treatment here is a continuous state master equation,

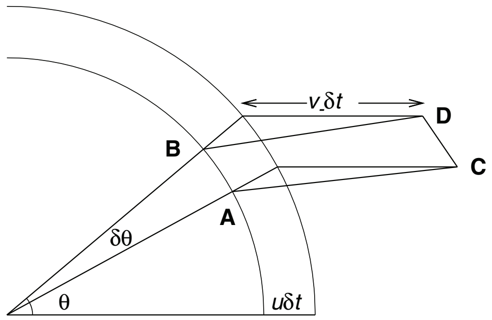

Fig. 2: A particle moves in the negative x-direction. The (almost) parallelogram ABDC denotes the initial positions that will collide in time $[0, \delta t]$, at location $[\theta, \theta + \delta\theta]$, taking the moving boundary into account.

similar to the linear Boltzmann equations of refs. [11,23] (but spatially homogeneous). Correlations between collisions are neglected (but can be included using results of ref. [21]; see the appendix), but due to the mixing (hence also ergodicity) property of the dynamics, a long sequence of collisions has the same effect as a Markov chain with the correct probability distribution.

The general form of a master equation is

$$f_t(v,t) = \int [p(v,v')f(v',t) - p(v',v)f(v,t)]\,\mathrm{d}v', \tag{5}$$

where subscript t (later v) is the partial derivative and $p(v, v', t)$ is the collision rate for a collision taking v' to v; it has explicit time dependence from the moving boundaries which is again suppressed. We need to find the probability of a collision taking $v_- \in [v', v' + \delta v']$ to $v_+ \in [v, v + \delta v]$ at a time in $[t, t + \delta t]$ by integrating the distribution over the set of trajectories with the appropriate collision.

For $r < r_I$ the cross-section is independent of ψ, so we take $\psi = \pi$; larger radii or different chaotic maps would need to take the ψ-dependence into account. The trajectory hits the scatterer at time t at a point $A(r(t)\cos\theta, r(t)\sin\theta)$; see fig. 2. A trajectory hitting the scatterer at angle $\theta + \delta\theta$ reaches it at $B(r(t)\cos(\theta + \delta\theta), r(t)\sin(\theta + \delta\theta))$. To reach the scatterer at $t + \delta t$, the particle at time t will be at $C(r(t + \delta t)\cos\theta + v_-\delta t, r(t+\delta t)\sin\theta)$ or $D(r(t+\delta t)\cos(\theta+\delta\theta)+v_-\delta t, r(t+\delta t)\sin(\theta + \delta\theta))$.

We need only the leading order in the perturbations, so ABDC is a parallelogram, with area $r(t)(u+v_- \cos\theta)\delta\theta\delta t$. We integrate over ψ to get

$$p(v_+, v_-) = -\frac{2r}{\mathcal{A}}(v_- \cos\theta + u)\left(\frac{\partial\theta}{\partial v_+}\right)_{v_-}, \tag{6}$$

where the final derivative comes because we used θ to denote the collision variable rather than v_+; they are related by eq. (3). The factor of two comes from considering both directions for each angle (see above), and the minus sign from the sign of the partial derivative. Substituting for θ, we find

$$p(v_+, v_-) = \frac{rv_+(v_+^2 - v_-^2)}{\mathcal{A}u\sqrt{8u^2(v_+^2 + v_-^2) - (v_+^2 - v_-^2)^2 - 16u^4}}. \tag{7}$$

Anticipating the expansion in powers of u, we now write $v_+ = v_- + 2su$ so that s ranges in the fixed interval $[0, 1]$, and use this in the master equation

$$\begin{aligned} f_t(v,t) \;=\; &\frac{r}{\mathcal{A}}\int_0^1 [\,p(v, v-2su)f(v-2su,t) \\ &- p(v+2su, v)f(v,t)]\,2u\mathrm{d}s. \end{aligned} \tag{8}$$

For very small velocities ($v < 2|u|$) we should modify the limits of integration to ensure that the arguments of p are both positive; however, in practice, this is not important as we are interested in long times after which the distribution is almost all at large velocities.

We now consider times of order unity, that is, the period of the oscillations. The master equation as it stands is not tractable, being explicitly time dependent. Noting again that for typical particle velocities $v \gg |u|$, we expand the right-hand side of the master equation in a power series in u, a Kramers-Moyal expansion [28] as used in ref. [11]. The functions f and p are expanded in powers of u, which then allows the integral to be performed, leading to

$$f_t = \frac{r}{\mathcal{A}}\left[-\pi u(f + vf_v) + \frac{8u^2vf_{vv}}{3} + O(u^3)\right]. \tag{9}$$

This is now used to determine $f(v, t)$ at long times. We note that when $r < r_I$, *i.e.* in the IH, IF and FH cases, $\dot{\mathcal{A}}/2 = -\pi ru$ is the term that appears in front of the first two terms on the right-hand side. Presumably this term is also $\dot{\mathcal{A}}/2$ for $r > r_I$, as in ref. [21], which gives a comparable equation; a detailed comparison is given in the appendix. Note that terms involving u^3 and higher are significant only for velocities of order $\sqrt{t}$ or less, thus they do not contribute to the main scaling, which is of order t.

We now come to the main issue with the oscillating volume. During each period, the particles make $O(v)$ collisions with the scatterer during each of the expanding and contracting phases, thus increasing and decreasing their speeds by $O(v)$ (with standard deviation $O(\sqrt{v})$). If we average eq. (9) by neglecting the u terms (which are full time derivatives if the time dependence of $f + vf_v$ can be ignored) we find $\bar{f}_t = 8Cv\bar{f}_{vv}/3$, where C is the average of $u^2/\mathcal{A}$, leading to $\bar{f}(v, t) = 9ve^{-3v/(8Ct)}/(64C^2t^2)$. However, this cannot capture the oscillations in f. Thus, we propose a more general ansatz, allowing v to scale with a bounded, but otherwise arbitrary 2π-periodic function $a(t)$:

$$f(v,t) = a(t)^2\frac{v}{t}e^{-a(t)v/t}, \tag{10}$$

where the prefactor $a(t)^2$ is required for normalisation, eq. (4). Substituting into eq. (9) gives an ODE involving the oscillatory r and u:

$$\frac{\mathrm{d}a}{\mathrm{d}t} = \left(t^{-1} - \frac{\pi ur}{\mathcal{A}}\right)a - \frac{8}{3t}\frac{u^2r}{\mathcal{A}}a^2. \tag{11}$$

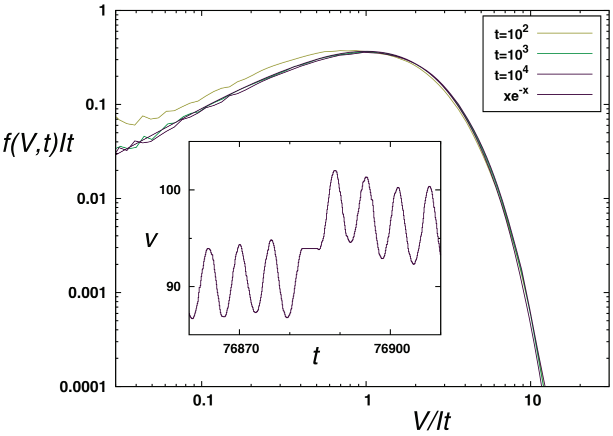

Fig. 3: (Colour on-line) Convergence to the distribution, eq. (14), for $R = 0.5$ (finite horizon). Inset: time dependence of the velocity for a single trajectory for $R = 0.3$ (infinite horizon). This step function is approximately sinusoidal except for jumps due to occasional long flights.

This is a Bernoulli equation, with solution

$$a(t) = t\frac{\sqrt{\mathcal{A}(t)}}{i(t)}, \qquad i(t) = \frac{8}{3}\int^t \frac{u^2 r}{\sqrt{\mathcal{A}}}\mathrm{d}t'. \tag{12}$$

Long-time behaviour is characterized by

$$I \equiv \lim_{t\to\infty}\frac{i(t)}{t} = \frac{4}{3\pi}\int_0^{2\pi}\frac{u^2 r}{\sqrt{\mathcal{A}}}\mathrm{d}t, \tag{13}$$

an elliptic integral depending on R and A that is easy to evaluate numerically [29]. Thus, our final expression for the velocity distribution function is

$$F(V,t) = \frac{V}{I^2t^2}e^{-V/(It)}, \tag{14}$$

where $V = v\sqrt{\mathcal{A}}$ and $F(V,t)\mathrm{d}V = f(v,t)\mathrm{d}v$. In contrast to this exponential form observed in similar systems [11,23], the relevant quantity V oscillates rapidly with respect to the velocities. More generally, in an adiabatic compression we expect the entropy to vary only slowly. Indeed for a two-dimensional ideal gas with only translational degrees of freedom, the entropy per particle is given by [30] $R\ln(mTa) + C$, where R and C are constants, m is the mass, T is the temperature and a the area per particle. Identifying T as proportional to v^2 we find that the entropy is just the logarithm of V with some constants. The importance of the entropy in forced systems was noted in ref. [31]; see also ref. [22].

This distribution is confirmed numerically in fig. 3 for $R = 0.5$ and $A = 0.03$, and so the FH regime. For this case the numerical integration gives $I \approx 0.001327658$. We simulate the full (not SWA) time-periodic Lorentz gas. Determining the time until the next collision thus involves the solution of a transcendental equation, using the robust quadratically convergent method proposed in [16]. A million initial conditions of particles are chosen using a Maxwell-Boltzmann distribution at a temperature of 10^{-4} consistent with $|u| < A = 0.03$. Particles which are very slow may not collide during the simulation time, and so delay the convergence to the limiting distribution. Note that $\mathcal{A}$ leads to a significant variation in v every cycle; this is clear in the inset, and would be visible in the distributions for different t if not incorporated correctly.

Next, we consider infinite horizon. Here, there is no separation between the collision and oscillation time scales, and the master equation cannot be applied; in general the velocity distribution is non-universal. We will however determine the scaling of velocity with time. There are two cases, I (pure infinite horizon) and IF (infinite-finite, also called dynamically infinite). For IF the time of free flights is bounded by the period, but since the velocity can be arbitrarily large, the distance is unbounded.

For both I and IF we will argue that the FA is of the form $v \sim t\ln t$. Physically, the more rapid acceleration is due to the particles making long flights while the scatterers are contracting, and so they miss the cooling phase of the cycle; see the inset of fig. 3. Some will do the opposite and miss the heating phase, but, as with a random walk, the overall effect of larger steps in energy per cycle is a higher rate of growth of the average energy.

In detail: The probability of a long flight of duration between τ and $\tau + \mathrm{d}\tau$ is (neglecting multiplicative constants) of order $(v\tau)^{-3}\mathrm{d}(v\tau) = v^{-2}\tau^{-3}\mathrm{d}\tau$ for $\tau \gg v^{-1}$, the typical flight time. See ref. [26] for an exact constant in the static case.

Collisions normally occur with a rate $\approx v$, so a long flight avoids a change of velocity $\approx v\tau$ to the particle, since u is at most of order unity. Thus, the perturbation $\delta\ln v = \delta v/v$ is of order τ. The effects are however effectively uncorrelated, so we add variances in proportion to their probability,

$$\sum(\delta\ln v)^2 \approx \int_{v^{-1}}^1 v^{-2}\tau^{-3}\tau^2\mathrm{d}\tau. \tag{15}$$

The lower limit of integration is the typical time v^{-1} and the upper can be taken as the largest time found in the trajectory; however, there is no extra velocity perturbation for free paths of time greater than the period (of order 1). Thus, we find that per collision the variance scales as $\ln v/v^2$. The number of collisions required to reach paths of order unity is about $v^2/\ln v$, which is less than the simulation time, noting that in the finite-horizon case FA is of order $v \sim t$.

Each particle thus undergoes a random walk in $\ln v$, taking a number of collisions $v^2/\ln v$, hence a time $v/\ln v$ to take each step. The total time for the trajectory is dominated by the largest value of v in the path, so that the velocity is typically of order $t\ln t$. This argument follows through for both infinite (I) and infinite/finite (IF) cases, although it is more pronounced (larger coefficient) in the former. Note the paradoxical effect in which the intermittency leads to long times without collisions, but is responsible for increasing the (collision-driven) FA.

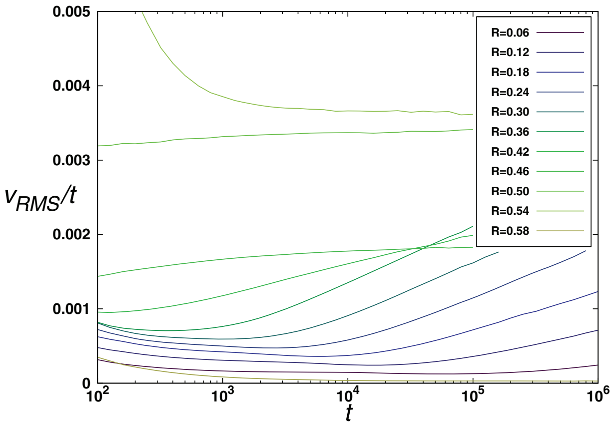

Fig. 4: (Colour on-line) Velocity growth for different values of R. The curves start horizontally ($v \sim t$), and those with $R < 0.45$, where the infinite horizon is noticeable, then increase linearly ($v \sim t \ln t$). The lowest curve, $R = 0.58$, is a billiard completely confined for the whole time, exhibiting the weakest Fermi acceleration.

We remark that the transport in velocity in both finite- and infinite-horizon cases is purely diffusive, *i.e.* free of a drift term, which would markedly alter the exponent of t, in contrast to the numerical results presented here. This means that the dynamics is almost certainly recurrent, eventually returning near its starting point on very long time scales.

The dependence of the FA on the radius (and hence the finite-/infinite-horizon status) is shown in fig. 4. The time regimes are (a) dominated by the initial Maxwell-Boltzmann distribution, (b) linear growth of v, (c) for I, increase as the logarithmic equation (15) starts to dominate the normal linear acceleration when there start to be several collisions per oscillation cycle. The linear growth in v is proportional to the cross-section (roughly R), thus the collision rate is roughly $R^2 t$ and the transition to several collisions per cycle occurs at roughly $t \sim R^{-2}$ for small R, as can be seen from the minima in fig. 4.

To summarise, we have demonstrated several new methods and effects for systems with periodic volume oscillations. The master equation approach can be applied to any time-dependent container for which the static dynamics is chaotic, specifically with integrable decay of correlations. The intermittent case, for example with non-integrable decay of correlations, does not appear to exhibit a universal velocity distribution and so it needs further study.

The FC parameter range, in which the particles are alternately confined and unconfined, is also unexplored. In particular, it would be interesting to investigate the many rapid collisions undertaken by a particle near where the two scatterers touch, a new "dynamical cusp" mode of intermittency. The possibility of an unbounded number of collisions suggests that since in each (approximately perpendicular) collision, a fixed quantity u is added to the velocity, the velocity itself can become unbounded in finite time for a small set of initial conditions, a further example of intermittency-enhanced acceleration.

Finally, physical experiments involve many other features —soft potentials, external fields, interparticle interactions and quantum effects. Our results suggest a thermodynamic approach, characterising particle distributions in terms of entropy.

* * *

The authors are grateful for support from Brazilian agencies FAPESP, FUNDUNESP and CNPq. This research was supported by resources supplied by the Center for Scientific Computing (NCC/GridUNESP) of the São Paulo State University (UNESP).

Appendix

Here we compare eq. (9) with the previous result of ref. [21]. The f_{vv} term in eq. (9) is of the same form as the diffusive term in ref. [21] (substituting energy $E = mv^2/2$ and mass $m = 1$), but has a different coefficient, for two reasons: ref. [21] neglects the effect of motion of the boundary on the collision rate ("aberration," fig. 2). In addition we assume the independence of collisions, good for the Lorentz gas except very close to r_I. In detail, eqs. (3.12), (3.16a), (3.22a) of ref. [21] give the same form as in eq. (9) but with $8u^2/3$ replaced by $4\sum_{j=-\infty}^{\infty} c_j$, where c_j is the autocorrelation of the function $u\cos\theta - \langle u\cos\theta\rangle$ in our notation, and here u is independent of the position. The main term is $4c_0 = (8/3 - \pi^2/4)u^2$, given (correctly) in eq. (A7) of ref. [21]. The other correlations are small, for example, the largest term for $r = 0.53$, just smaller than r_I, is $4c_3 \approx 0.008$. Numerical simulations (fig. 3) are consistent with 8/3 plus undetectable correlation corrections, but not with $8/3 - \pi^2/4$. If desired, we can incorporate the other c_j into our approach directly, by increasing the coefficient to $8/3 + 4\sum_{j\neq 0} c_j$.

REFERENCES

[1] Gilary I., Moiseyev N., Rahav S. and Fishman S., *J. Phys. A: Math. Theor.*, **36** (2003) L409.
[2] Gelfreich V., Rom-Kedar V., Shah K. and Turaev D., *Phys. Rev. Lett.*, **106** (2011) 074101.
[3] Salger T., Kling S., Hecking T., Geckeler C., Morales-Molina L. and Weitz M., *Science*, **326** (2009) 1241.
[4] Ospelkaus C., Langer C. E., Amini J. M., Brown K. R., Leibfried D. and Wineland D. J., *Phys. Rev. Lett.*, **101** (2008) 090502.
[5] Shevchenko I. I., *New Astron.*, **16** (2011) 94.
[6] Leonel E. D., da Costa D. R. and Dettmann C. P., *Phys. Lett. A*, **376** (2012) 421.
[7] Fermi E., *Phys. Rev.*, **75** (1949) 1169.
[8] Bunin G., D'Alessio L., Kafri Y. and Polkovnikov A., *Nat. Phys.*, **7** (2011) 913.
[9] Karlis A. K., Diakonos F. K., Petri C. and Schmelcher P., *Phys. Rev. Lett.*, **109** (2012) 110601.

[10] Karlis A. K., Diakonos F. K. and Constantoudis V., *Chaos*, **22** (2012) 026120.
[11] D'Alessio L. and Krapivsky P. L., *Phys. Rev. E*, **83** (2011) 011107.
[12] Jarzyński C. and Świątecki W., *Nucl. Phys. A*, **552** (1993) 1.
[13] Karlis A. K., Papachristou P. K., Diakonos F. K., Constantoudis V. and Schmelcher P., *Phys. Rev. E*, **76** (2007) 016214.
[14] Loskutov A., Ryabov A. and Akinshin L., *J. Exp. Theor. Phys.*, **89** (1999) 966.
[15] Loskutov A., Ryabov A. B. and Akinshin L. G., *J. Phys. A: Math. Theor.*, **33** (2000) 7973.
[16] Dettmann C. P. and Leonel E. D., *Physica D*, **241** (2012) 403.
[17] Lenz F., Diakonos F. K. and Schmelcher P., *Phys. Rev. Lett.*, **100** (2008) 014103.
[18] Batisti B. and Robnik M., *J. Phys. A: Math. Theor.*, **44** (2011) 365101.
[19] Oliveira D. F. M., Vollmer J. and Leonel E. D., *Physica D*, **240** (2011) 389.
[20] Błocki J., Brut F. and Świątecki W. J., *Nucl. Phys. A*, **554** (1993) 107.
[21] Jarzyński C., *Phys. Rev. E*, **48** (1993) 4340.
[22] Błocki J., Jarzyński C. and Świątecki W. J., *Nucl. Phys. A*, **599** (1996) 486.
[23] Bouchet F., Cecconi F. and Vulpiani A., *Phys. Rev. Lett.*, **92** (2004) 040601.
[24] Gradenigo G., Puglisi A., Sarracino A. and Marconi U. M. B., *Phys. Rev. E*, **85** (2012) 031112.
[25] Kruis H. V., Panja D. and van Beijeren H., *J. Stat. Phys.*, **124** (2006) 823.
[26] Dettmann C. P., *J. Stat. Phys.*, **146** (2012) 181.
[27] Evans D. and Morriss G., *Statistical Mechanics of Nonequilibrium Liquids* (Cambridge University Press) 2008.
[28] Risken H. and Vollmer H. D., *Z. Phys. B Condens. Matter*, **66** (1987) 257.
[29] Weideman J. A. C., *Am. Math. Mon.*, **109** (2002) 21.
[30] Kemball C., *Proc. R. Soc. London, Ser. A*, **187** (1946) 73.
[31] Ott E., *Phys. Rev. Lett.*, **42** (1979) 1628.